

REVIEW

Imaging ‘the lost tribe’: a review of adolescent cancer imaging. Part 2: imaging of complications of cancer treatment

I. Zerizer and P.D. Humphries

University College London Hospital NHS Trust, 235 Euston Road, London, NW1, UK

Corresponding address: Dr P.D. Humphries, Specialist X-ray, Podium Level 2, University College London Hospital NHS Trust, 235 Euston Road, London, NW1, UK.

Email: paul.humphries@ulch.nhs.uk

Date accepted for publication 2 September 2009

Abstract

Adolescent cancers are treated with a host of chemotherapy agents, radiotherapy and stem cell transplantation. The complications of these treatments may contribute significantly to the morbidity and mortality in this age group, with imaging playing a role in identifying some of these complications. This second article reviews the imaging of acute and early complications relating to adolescent cancer treatment, many of which may also be seen in the treatment of paediatric patients. Late effects involving endocrine and reproductive systems or psychosocial considerations are not discussed in this paper, although these are clearly important issues in long-term survivors.

Keywords: Adolescent; oncology; complications; imaging.

Pulmonary complications

Pulmonary complications in patients undergoing cancer treatment are common, estimated at 40–60%; the most common and important are infections and drug toxicity^[1].

Pulmonary infections

Pulmonary infections are a major cause of morbidity and mortality in immunosuppressed patients. It has been reported that up to 70% of patients undergoing chemotherapy and 11–43% undergoing bone marrow transplantation will have a pulmonary infection^[1].

Aspergillus is the most common causative organism, infecting the airways, resulting initially in bronchopneumonia. The plain chest radiograph may be normal at this stage but nodular changes or consolidation will become apparent as the disease progresses. As the *Aspergillus* organisms invade the bronchopulmonary vasculature resulting in angioinvasive aspergillosis, multiple areas of consolidation secondary to infarction

become apparent^[1]. Computed tomography (CT) and plain radiographs are more than 90% accurate for the diagnosis of invasive aspergillosis^[1]. The radiographic findings include multiple nodules demonstrating the halo sign (a rim of ground-glass opacification), rapidly enlarging, spherical, masklike opacities and cavitating lesions with an air crescent sign. Immunosuppressed patients are also susceptible to pulmonary infection secondary to *Candida*, cytomegalovirus and herpes simplex virus and many other opportunistic pathogens. The radiographic findings are non-specific and therefore a high index of suspicion should always be maintained^[1].

Pulmonary toxicity

Patients are at increased risk of developing pulmonary reactions secondary to chemotherapy agents.

Methodrextate pulmonary toxicity is well documented in the literature, with incidence from 0.3 to 12% reported^[2]. Symptoms usually develop within weeks of the onset of treatment and include fever, dyspnoea, persistent non-productive cough, and/or rash. The disease then



Figure 1 Axial CT section demonstrating subpleural ground-glass change in a patient with NSIP.

develops rapidly into an infiltrative lung pattern, resulting in respiratory failure. Severe hypoxemia is consistently present. Mild peripheral eosinophilia is present in 40% of patients^[1]. Non-specific interstitial pneumonia (NSIP) is the most common manifestation of methotrexate-induced lung disease (Fig. 1). Bronchiolitis obliterans-organizing pneumonia (BOOP)/cryptogenic organizing pneumonia (COP), interstitial pneumonitis, and non-cardiogenic pulmonary oedema may also be seen^[1]. Chest radiographs reveal ill-defined reticular opacities, ground-glass opacity, or consolidation with a basal prominence. The most common finding on high-resolution CT (HRCT) is ground-glass change. Diffuse bilateral infiltrates or dense consolidation with air bronchograms are also recognised. If COP is present, nodular areas of consolidation, centrilobular nodules, branching linear opacities, and bronchial dilatation can also be found (Fig. 2)^[3]. The pulmonary changes of methotrexate toxicity are usually reversible, unlike other cytotoxic drugs^[1].

Cyclophosphamide is used in the treatment of various forms of leukaemia and lymphomas and before bone marrow or stem cell transplantation. The rate of cyclophosphamide-induced pulmonary toxicity is approximately 1%. Risk factors for developing pulmonary toxicity include concomitant radiation therapy, use of other cytotoxic agents known to be associated with lung toxicity (e.g. bleomycin), and exposure to high concentrations of oxygen^[4]. There are 2 clinical patterns of pulmonary toxicity associated with cyclophosphamide: an acute pneumonitis that occurs early in the course of treatment and a chronic, progressive, fibrotic process that may occur after prolonged therapy. The acute form can be reversible if cyclophosphamide is discontinued and steroid therapy commenced early. Chronic cyclophosphamide pneumonitis is regarded as an irreversible entity, which takes the form of progressive pulmonary fibrosis with respiratory failure^[4]. On plain radiographs and HRCT bilateral reticular or nodular diffuse opacities are the hallmarks of early- and late-onset pulmonary



Figure 2 Axial CT section demonstrating multifocal ground-glass and consolidation, with an area of peribronchial linear consolidation extending to the left oblique fissure (arrow), typical of cryptogenic organizing pneumonia.

toxicity. In the acute stage of pneumonitis, the abnormalities may only be detected on HRCT, which reveals ground-glass opacities predominantly in the periphery of the upper lobes. The radiographic opacities of chronic pneumonitis have a more fibrotic appearance involving mostly mid and upper lung regions. Pneumothorax may develop as a complication.

Bleomycin is used for the treatment of head and neck carcinomas, germ cell tumours, and lymphoma, and can lead to pulmonary toxicity in up to 10% of cases^[5]. Risk factors for lung toxicity are the same as those associated with cyclophosphamide toxicity and, in addition, combination therapy with cyclophosphamide or granulocyte-colony stimulating factor and renal failure^[6]. A variety of adverse reactions to bleomycin have been reported, including chronic interstitial fibrosis, hypersensitivity-type disease, and COP. Pneumonitis with pulmonary fibrosis can develop 6–8 weeks after the onset of treatment^[7]. Chest radiographs may show reticulation and ground-glass opacity; consolidation with a predominant subpleural and lower lobe predominance with generalized loss of lung volume may also occur. HRCT findings reflect the pattern of pulmonary toxicity but sometimes reveal multiple pulmonary nodules, which may mimic metastatic disease but have the histologic characteristics of COP^[3].

Central nervous system complications

Central nervous system (CNS) complications in paediatric oncology are well recognised following chemotherapy and stem cell transplantation. However, there are a lack of clinical studies documenting its incidence and clinical pattern, particularly in adolescents.

A single-centre retrospective analysis of CNS complications in 950 paediatric patients treated between

1992 and 2004 by chemotherapy or haematopoietic stem transplantation revealed that infection (26.8%) was the most common complication, followed by toxicity (25.6%), neoplasms (13.4%), vascular (10.9%) and metabolic disturbances (8.5%)^[81]. The mechanism remained unclear in 14% of patients. The mortality from CNS complications was estimated at 23.7%. Neoplastic disorders had the worst prognosis, with 50% mortality; metabolic complications fared better with no deaths seen in this group.

Infection

The incidence of cerebral infections complicating chemotherapy or stem cell transplant varies between 2 and 14%, the most common causative organism being *Aspergillus* (30–50%)^[81]. Various other pathogens are also found including *Pseudomonas*, *Listeria*, human herpes virus 6, herpes zoster and toxoplasmosis.

The radiological manifestations of CNS infections can be divided into the following pathologic entities: (i) focal lesions, (ii) invasive sinusitis, (iii) cerebral infarction, (iv) demyelination, (v) encephalitis and (vi) meningitis/hydrocephalus^[81].

Cerebral aspergillosis is responsible for more than 90% of CNS abscesses and focal lesions in the immunocompromised^[81]. On CT the lesions are typically found in the basal ganglia and juxtacortical white matter and appear as areas of low attenuation with little or no mass effect and no enhancement. On magnetic resonance imaging (MRI), these lesions are of intermediate signal intensity on T2-weighted imaging with a rim of higher signal. Wedge-shaped lesions in the cerebral cortex can also be found as a result of infarction secondary to occlusion of the intracerebral vessels by the aspergillus hyphae^[91].

Cerebral toxoplasmosis should also be considered in the differential diagnosis of intracerebral focal lesions in immunocompromised patients, although this complication is less commonly encountered in this group of patients. Lesions are typically found in the basal ganglia and enhance post contrast^[91].

Invasive fungal sinusitis is a severe infection of the paranasal sinuses that can involve all of the head and neck structures. The infection is fatal unless aggressive surgical debridement and systemic antifungals are instituted. The most common causative organisms are *Aspergillus* and mucormycosis^[81]. On CT, early diagnosis of fungal sinusitis is suggested by the presence of opacification in one or more paranasal sinus in the absence of a fluid level. Bone destruction becomes more apparent as the disease progresses with intracranial and intraorbital extension. MRI is more sensitive for the detection of intraorbital and intracranial extension^[81].

Viral infection may cause various clinical entities, ranging from infarctions secondary to vasculitis (e.g. leptomeningeal vasculopathy seen with herpes zoster), encephalitis (seen with herpes viruses, cytomegalovirus and Epstein–Barr virus) and progressive multifocal

leucoencephalopathy, a demyelinating disorder secondary to JC virus (although there have been reports of progressive multifocal leucoencephalopathy (PML) secondary to chemotherapy)^[9,101].

CNS drug toxicity

Multiple chemotherapy agents are responsible for CNS complications. The frequency of CNS complications varies between 1.6 and 10.3%^[81]. Cyclosporin is the most common cause of such complications, which typically result in symmetric signal change in the cortex and juxtacortical white matter of the posterior cerebral circulation^[111]. Methotrexate CNS toxicity leads to a symmetric leucoencephalopathy, involving the subcortical white matter (Fig. 3) and basal ganglia. A severe form of necrotising leucoencephalopathy can also be seen with multiple foci of T2 hyperintensity with avid contrast enhancement^[112]. Other chemotherapy agents that can induce CNS toxicity include cytarabin, ifosfamide and vincristine^[113].

Cranial irradiation can potentiate the CNS toxicity of chemotherapy agents and produce diffuse signal change predominantly within the periventricular white matter associated with cerebral atrophy and focal lesions that resemble small vessel infarcts^[114].

Secondary CNS neoplasms

Secondary brain malignancy occurs in up to 5% of patients. The most common malignancy is high-grade glioma followed by primitive neuroectodermal tumours. Meningiomas and low-grade gliomas also occur^[81]. The most important predictors for the development of secondary malignancy are CNS leukaemia and cranial irradiation dose.

Thromboembolic disease

Cerebral infarction results from various causes, including sinus venous occlusive disease (Fig. 4), tumour emboli, cytotoxic and cerebral irradiation and infections (as described earlier). Cerebral infarction has been reported in 6–38% of patients following chemotherapy and bone marrow transplant^[81].

CNS metabolic effects

Metabolic abnormalities may also be seen during the treatment of patients with chemotherapy, including hyperosmolar hyperglycaemia, lactic acidosis, vitamin B₁ deficiency. Extrapontine myelinosis may be seen, typically presenting with hyperintense lesions in the basal ganglia with restricted diffusion and lack of enhancement. Pontine lesions may also be encountered.

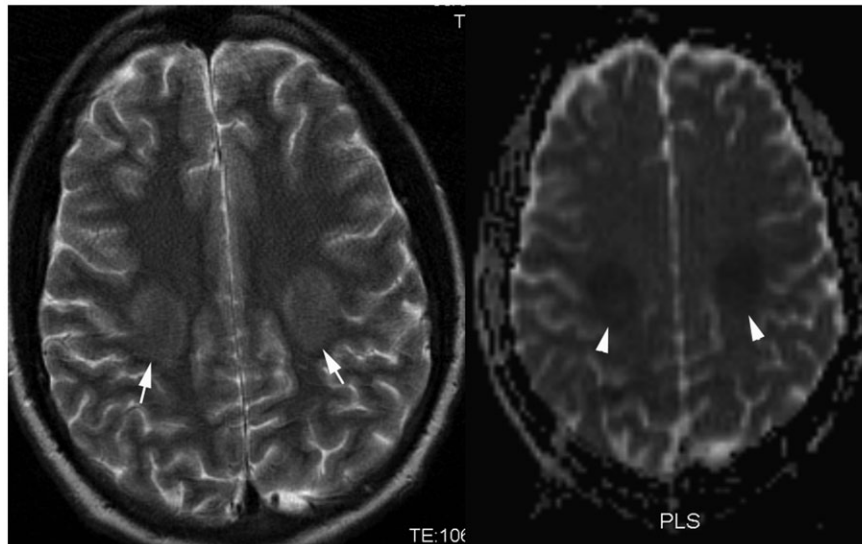


Figure 3 Methotrexate leucoencephalopathy. Axial T2-weighted MRI (TR 4350, TE 106 ms) showing hyperintense foci within both centra semiovale (short arrows), with corresponding restricted diffusion on apparent diffusion coefficient map (arrow heads).

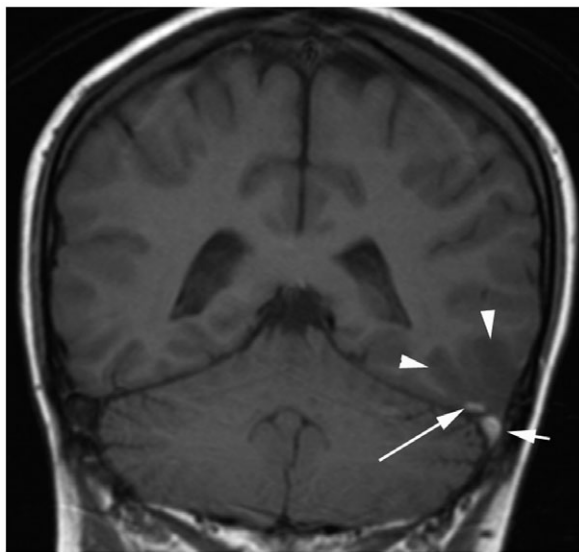


Figure 4 Coronal T1-weighted MRI (TR 472, TE 9.7 ms) showing thrombus within the left transverse sinus (short arrow) and a temporal lobe cortical vein (long arrow), with swelling of the left temporal lobe (arrowheads), consistent with an infarct.

Musculoskeletal complications

Osteonecrosis

Osteonecrosis of the bone is seen as a complication of treatment of acute lymphoblastic leukaemia (ALL) and lymphoma, usually reported in children following corticosteroid therapy. In general terms osteonecrosis

involving the metaphysis or diaphyseal regions of bone are referred to as medullary bone infarcts, and lesions involving the epiphyses are referred to as avascular necrosis (AVN), both being secondary to cellular death. AVN is typically painful; medullary bone infarcts may be clinically silent. The spectrum of osteonecrosis in adolescents and young adults is poorly documented in the literature.

A recent study examined the incidence of AVN in ALL patients aged 15–55 years. The highest incidence of AVN, estimated at 15%, was found in patients less than 20 years old^[15]. Another report on AVN in children with ALL also found a higher incidence in older children^[16]. Strauss *et al.*^[16] also predicted that as an increasing number of younger adults receive ALL treatment according to paediatric rather than adult protocols with an associated higher dose intensity of steroids, there would be an increased incidence of AVN in adolescents. The proposed mechanism of corticosteroid-induced AVN in adolescents attributes physiologic changes, such as epiphyseal closure and changes in circulating hormone levels in the maturing bones of adolescents, as the most important factors rendering bones susceptible to steroid-induced changes.

Most cases of AVN in childhood occur within the first 2 years after diagnosis; cases in adolescents and young adults tend to occur more than 2 years after the start of ALL therapy, hence a high index of suspicion during post-therapy follow-up should be maintained^[15,16]. The joints most commonly affected are the hips and shoulders although involvement of multiple joints has also been described^[15].

Plain radiographs are normal in the acute stages and the earliest changes are only seen after several weeks.

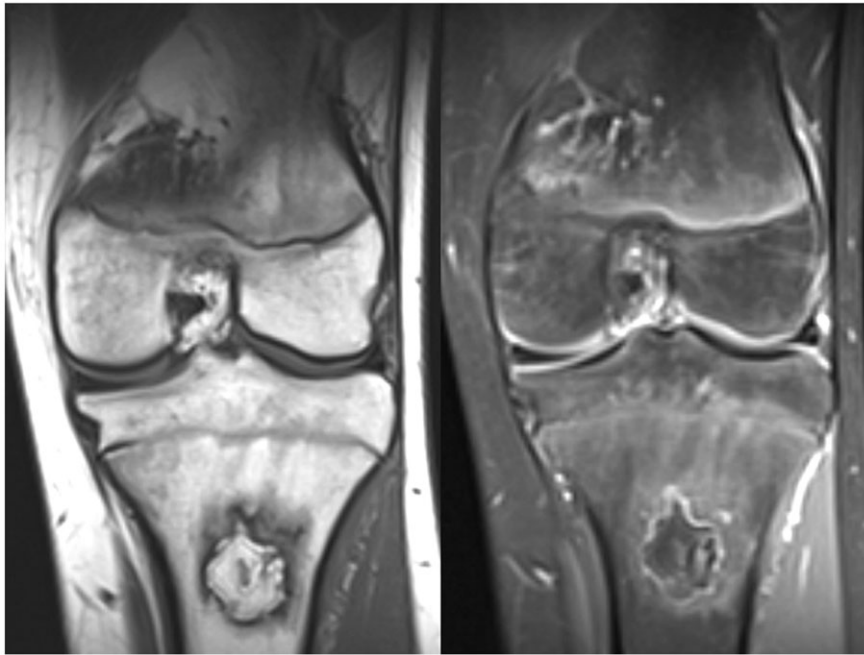


Figure 5 Coronal T1 (TR 470, TE 11 ms) and post gadolinium T1 fat saturated images of a proximal tibial infarct in a patient with acute lymphoblastic leukaemia, showing the classic enhancing serpiginous margin.

These include trabecular mottling, followed by focal sclerosis and osteopenia. After a few months, radiolucencies are demonstrated reflecting subchondral collapse. The joint space is preserved at this stage. Later there is articular surface flattening and sclerosis followed by collapse, joint space narrowing and degenerative changes.

The reported frequency of osteonecrosis with MRI screening varies from 0 to 44% depending on the type of therapy administered. The sensitivity of MRI is high for the detection of AVN ranging from 90 to 95%; use of gadolinium increases early detection^[17]. MRI findings of osteonecrosis include decreased signal intensity in the subchondral region on T1- and T2-weighted images, suggesting oedema in early disease. The next stage is characterized by a reparative process (reactive zone) and shows low signal intensity on T1-weighted scans and high signal intensity on T2-weighted scans. A serpentine margin with low and high peripheral zones on T2-weighted spin echo images (the so-called double line sign) is characteristic; classically there is enhancement following gadolinium administration on T1-weighted images (Fig. 5). Osteonecrosis on T2-weighted images appears as focal areas of increase signal. Advanced AVN is characterized by deformity of the articular surface and by calcification, which are easily detected with radiography and CT.

Planar bone scintigraphy can also be used for the detection of AVN with a reported sensitivity of 55%^[18]. The appearances are non-specific with areas of reduced activity reflecting avascularity and areas of increased activity implying increased osteoblastic activity within

revascularisation or degenerative changes secondary to joint collapse. Bone scintigraphy equipped with a pinhole collimator has greater sensitivity for diagnosing AVN than bone scintigraphy using a high-resolution parallel-hole collimator^[19]. The appearance of medullary bone infarction on bone scintigraphy varies depending on the timing of the study in relation to the insult. Initially, in the first few days after infarction, photopenia or normal uptake is seen. Later increased uptake is observed, secondary to revascularisation via periosteal vessels. Old bone infarcts vary in appearance, depending on the degree of revascularisation. In areas of adequate revascularisation, the appearance may return to normal after a few months. Areas of avascular bone are seen as persistent photopenic foci.

Hepatic veno-occlusive disease

Hepatic veno-occlusive disease (VOD) is a well-recognised complication of haematopoietic stem cell transplant, occurring in approximately a quarter of all paediatric and young adult patients^[20], but can also be seen in the setting of Wilms tumour treatment (an uncommon tumour in the adolescent population), with an incidence of approximately 5%; abdominal irradiation is a risk factor for its development^[21]. There have been reports of VOD developing during the treatment of other malignancies including rhabdomyosarcoma^[22] and CNS tumours^[23]. A pre-existing structural abnormality, such as a metastasis associated with a solid tumour, also predisposes to the condition^[24].



Figure 6 Axial contrast-enhanced portal venous phase CT showing central enhancement, collateral vessels (short arrows) and ascites (arrow head) in a patient with BCS. The hepatic veins could not be visualised in this case.

Hepatic VOD manifests typically with tender hepatomegaly, fluid retention, weight gain and jaundice. Pathologically the primary event is injury to sinusoidal endothelial cells, leading ultimately to narrowing and fibrosis of central veins with resulting obstruction of liver blood flow and is more appropriately termed sinusoidal obstruction syndrome (SOS) rather than VOD^[25]. Clinical diagnostic criteria (Seattle and Baltimore criteria) are generally used to diagnose VOD/SOS^[26,27], although liver biopsy remains the gold standard but has attendant risks in thrombocytopenic patients.

On ultrasound examination it has been suggested that reversal of flow within a segment of the portal vein suggests the diagnosis of VOD/SOS^[28], however the liver frequently appears normal. The main role of imaging is to exclude other conditions that mimic VOD/SOS, for example Budd–Chiari syndrome (BCS), in which hepatic vein Doppler traces may be abnormal and comma-shaped collateral vessels can be seen. Non-visualisation of the hepatic vein/inferior vena cava (IVC) confluence may also be observed in BCS (Fig. 6). Given that VOD/SOS and BCS cause obstruction to liver outflow, it is perhaps unsurprising that there are reports of similar findings in both conditions on MRI^[29]. The most important differentiator between the conditions is patency of the major hepatic veins and IVC in VOD/SOS.

Pancreatitis

Acute pancreatitis is an uncommon complication of chemotherapy. Causative agents include L-asparaginase, cisplatin, high-dose cytosine arabinoside, corticosteroids, cyclophosphamide and ifosfamide^[30]. The diagnosis of acute pancreatitis may be suggested on ultrasound, which shows inflammation of the pancreas with focal



Figure 7 Axial contrast-enhanced CT section in a patient with acute pancreatitis complicating L-asparaginase therapy, showing areas of pancreatic necrosis (short arrows) and marked peripancreatic inflammatory change (long arrow).

reduced echogenicity and possible surrounding free fluid. Ultrasound can be used during follow-up to detect complications such as pseudocysts. Despite the associated radiation burden, CT is probably the most useful modality in the setting of acute pancreatitis (Fig. 7), with higher sensitivity and specificity for diagnosis and detection of complications, particularly pseudoaneurysms that can be missed on ultrasound.

Conclusion

The complications seen in adolescent patients undergoing cancer treatment are varied. The relative frequency of treatment-related complications in paediatric and adolescent patients is not well documented and this data would be of interest to adapt strategies to prevent or ameliorate the effects of the most frequent complications within the two groups of patients. This review provides an overview of the potential role imaging has to play in the management of adolescent patients who have cancers, beyond diagnosis, staging and response assessment.

References

- [1] Rosenow III EC, Limper AH. Drug-induced pulmonary disease. *Semin Respir Infect* 1995; 10: 86–95.
- [2] Imokawa S, Colby TV, Leslie KO, Helmers RA. Methotrexate pneumonitis: review of the literature and histopathological findings in nine patients. *Eur Respir J* 2000; 15: 373–81. doi:10.1034/j.1399-3003.2000.15b25.x. PMID:10706507.
- [3] Kuhlman JE. The role of chest computed tomography in the diagnosis of drug-related reactions. *J Thorac Imaging* 1991; 6: 52–61.
- [4] Hamada K, Nagai S, Kitaichi M, *et al.* Cyclophosphamide-induced late-onset lung disease. *Intern Med* 2003; 42: 82–7. doi:10.2169/internalmedicine.42.82. PMID:12583625.

- [5] Balikian JP, Jochelson MS, Bauer KA, *et al.* Pulmonary complications of chemotherapy regimens containing bleomycin. *AJR Am J Roentgenol* 1982; 139: 455–61.
- [6] Toledo CH, Ross WE, Hood CI, Block ER. Potentiation of bleomycin toxicity by oxygen. *Cancer Treat Rep* 1982; 66: 359–62.
- [7] Daba MH, El Tahir KE, Al Arifi MN, Gubara OA. Drug-induced pulmonary fibrosis. *Saudi Med J* 2004; 25: 700–6.
- [8] Schmidt K, Schulz AS, Debatin KM, Friedrich W, Classen CF. CNS complications in children receiving chemotherapy or hematopoietic stem cell transplantation: retrospective analysis and clinical study of survivors. *Pediatr Blood Cancer* 2008; 50: 331–6. doi:10.1002/pbc.21237.
- [9] Connolly RM, Doherty CP, Beddy P, O'Byrne K. Chemotherapy induced reversible posterior leukoencephalopathy syndrome. *Lung Cancer* 2007; 56: 459–63. doi:10.1016/j.lungcan.2007.01.012. PMID:17316891.
- [10] Coley SC, Jäger HR, Szydlo RM, Goldman JM. CT and MRI manifestations of central nervous system infection following allogeneic bone marrow transplantation. *Clin Radiol* 1999; 54: 390–7. doi:10.1053/crad.1999.0200. PMID:10406341.
- [11] Takahata M, Hashino S, Izumiyama K, Chiba K, Suzuki S, Asaka M. Cyclosporin A-induced encephalopathy after allogeneic bone marrow transplantation with prevention of graft-versus-host disease by tacrolimus. *Bone Marrow Transplant* 2001; 28: 713–5. doi:10.1038/sj.bmt.1703221. PMID:11704797.
- [12] Kellie SJ, Chaku J, Lockwood LR, O'Regan P, Waters KD, Wong CK. Late magnetic resonance imaging features of leukoencephalopathy in children with central nervous system tumours following high-dose methotrexate and neuraxis radiation therapy. *Eur J Cancer* 2005; 41: 1588–96. doi:10.1016/j.ejca.2005.02.024. PMID:16026694.
- [13] Sioka C, Kyritsis AP. Central and peripheral nervous system toxicity of common chemotherapeutic agents. *Cancer Chemother Pharmacol* 2009; 63: 761–7. doi:10.1007/s00280-008-0876-6. PMID:19034447.
- [14] Lai R, Abrey LE, Rosenblum MK, DeAngelis LM. Treatment-induced leukoencephalopathy in primary CNS lymphoma: a clinical and autopsy study. *Neurology* 2004; 62: 451–6.
- [15] Patel B, Richards SM, Rowe JM, Goldstone AH, Fielding AK. High incidence of avascular necrosis in adolescents with acute lymphoblastic leukaemia: a UKALL XII analysis. *Leukemia* 2008; 22: 308–12. doi:10.1038/sj.leu.2405032. PMID:17989709.
- [16] Strauss AJ, Su JT, Dalton VM, Gelber RD, Sallan SE, Silverman LB. Bony morbidity in children treated for acute lymphoblastic leukemia. *J Clin Oncol* 2001; 19: 3066–72.
- [17] Ribeiro RC, Fletcher BD, Kennedy W, *et al.* Magnetic resonance imaging detection of avascular necrosis of the bone in children receiving intensive prednisone therapy for acute lymphoblastic leukemia or non-Hodgkin lymphoma. *Leukemia* 2001; 15: 891–7. doi:10.1038/sj.leu.2402139. PMID:11417473.
- [18] Oshima M, Yoshihara Y, Ito K, Asai H, Fukatsu H, Sakuma S. Initial stage of Legg-Calve-Perthes disease: comparison of three-phase bone scintigraphy and SPECT with MR imaging. *Eur J Radiol* 1992; 15: 107–12. doi:10.1016/0720-048X(92)90133-T. PMID:1425743.
- [19] Naito M, Ogata K, Moriguchi H. Quantitative bone scanning of the hip. Comparison between the perfusion and static phases. *Int Orthop* 1996; 20: 311–4. doi:10.1007/s002640050084. PMID:8930724.
- [20] Reiss U, Cowan M, McMillan A, Horn B. Hepatic venoocclusive disease in blood and bone marrow transplantation in children and young adults: incidence, risk factors, and outcome in a cohort of 241 patients. *J Pediatr Hematol Oncol* 2002; 24: 746–50. doi:10.1097/00043426-200212000-00013. PMID: .
- [21] Czuderna P, Katski K, Kowalczyk J, *et al.* Venooclusive liver disease (VOD) as a complication of Wilms' tumour management in the series of consecutive 206 patients. *Eur J Pediatr Surg* 2000; 10: 300–3. doi:10.1055/s-2008-1072380. PMID:11194540.
- [22] Sulis ML, Bessmertny O, Granowetter L, Weiner M, Kelly KM. Venooclusive disease in pediatric patients receiving actinomycin D and vincristine only for the treatment of rhabdomyosarcoma. *J Pediatr Hematol Oncol* 2004; 26: 843–6.
- [23] Elli M, Pinarli FG, Dagdemir A, Acar S. Venooclusive disease of the liver in a child after chemotherapy for brain tumor. *Pediatr Blood Cancer* 2006; 46: 521–3. doi:10.1002/pbc.20338.
- [24] Ayash LJ, Hunt M, Antman K, *et al.* Hepatic venooclusive disease in autologous bone marrow transplantation of solid tumors and lymphomas. *J Clin Oncol* 1990; 8: 1699–706.
- [25] DeLeve LD, Shulman HM, McDonald GB. Toxic injury to hepatic sinusoids: sinusoidal obstruction syndrome (venoocclusive disease). *Semin Liver Dis* 2002; 22: 27–42. doi:10.1055/s-2002-23204.
- [26] McDonald GB, Sharma P, Matthews DE, Shulman, Thomas ED. Venooclusive disease of the liver after bone marrow transplantation: diagnosis, incidence, and predisposing factors. *Hepatology* 1984; 4: 116–22. doi:10.1002/hep.1840040121. PMID:6363247.
- [27] Jones RJ, Lee KS, Beschoner WE, *et al.* Venooclusive disease of the liver following bone marrow transplantation. *Transplantation* 1987; 44: 778–83.
- [28] Yoshimoto K, Ono N, Okamura T, Sata M. Recent progress in the diagnosis and therapy for venooclusive disease of the liver. *Leuk Lymphoma* 2003; 44: 229–34. doi:10.1080/1042819021000029704. PMID: .
- [29] Mortelet KJ, Van Vlierberghe H, Wiesner W, Ros PR. Hepatic venooclusive disease: MRI findings. *Abdom Imaging* 2002; 27: 523–6.
- [30] Izraeli S, Adamson PC, Blaney SM, Balis FM. Acute pancreatitis after ifosfamide therapy. *Cancer* 1994; 74: 1627–8. doi:10.1002/1097-0142(19940901)74:5<1627::AID-CNCR2820740522>3.0.CO;2-U. PMID:8062195.